Journal of Power Sources 201 (2012) 59–65

Contents lists available at SciVerse ScienceDirect

Journal of Power Sources

journal homepage: www.elsevier.com/locate/jpowsour

Effects of operating conditions on internal resistances in enzyme fuel cells studied via electrochemical impedance spectroscopy

Doug Aaron[a], Abhijeet P. Borole[b,*], Sotira Yiacoumi[a], Costas Tsouris[a,b,*,1]

[a] School of Civil and Environmental Engineering Georgia Institute of Technology, Atlanta, GA 30332, United States
[b] Oak Ridge National Laboratory, Oak Ridge, TN 37831, United States

ARTICLE INFO

Article history:
Received 1 September 2011
Received in revised form 27 October 2011
Accepted 30 October 2011
Available online 6 November 2011

Keywords:
Enzyme fuel cell
Electrochemical impedance spectroscopy
Laccase

ABSTRACT

Enzyme fuel cells (EFCs) offer some advantages over traditional precious-metal-catalyzed fuel cells, such as polymer electrolyte membrane fuel cells (PEMFCs). However, EFCs exhibit far less power output than PEMFCs and have relatively short life spans before materials must be replaced. In this work, electrochemical impedance spectroscopy (EIS) is used to analyze the internal resistances throughout the EFC at a variety of operating conditions. EIS analysis is focused primarily on the resistances of the anode, solution/membrane, and cathode. Increased enzyme loading results in improved power output and reductions in internal resistance. Conditions are identified for which enzyme loading does not limit the EFC performance. EIS experiments are also reported for EFCs operated continuously for 2 days; power output declines sharply over time, while all internal resistances increase. Drying of the cathode and enzyme/mediator degradation are believed to have contributed to this behavior. Finally, experiments are performed at varying air-humidification temperatures. Little effect on internal resistances or power output is observed. However, it is anticipated that increased air humidification can improve longevity by delivering more water to the cathode. Improvements to the enzymatic cathode are needed for EFC development. These improvements need to focus on improving transport rather than increasing enzyme loading.

Published by Elsevier B.V.

1. Introduction

Enzyme fuel cells (EFCs) are a relatively novel type of fuel cells. EFCs use enzymes as catalysts. These enzymes are less costly than precious metal catalysts and operate at lower temperatures [1]. Such a replacement can drastically decrease the cost of fuel cell materials. Two more benefits stem from the specificity of enzymes: first, multiple fuels (not just hydrogen) can be used if the appropriate enzyme is selected [2,3]; second, the fuel cell geometry can be simplified because enzymes can be sufficiently specific that separation materials will not be required to chemically isolate the anode and cathode [4]. These aspects of EFCs afford them considerable economic potential for providing low-temperature power based on a variety of fuels. However, the use of EFCs is not without obstacles. Hudak et al. [5] noted that significant power loss is observed over time; contributing causes include enzyme degradation, mediator degradation, and cathode drying. In addition to these longevity issues, even the highest-power-density EFCs produce orders of magnitude less power than polymer-electrolyte-membrane fuel cells (PEMFCs) at similar conditions. Power densities in the range of 10–85 W m^{-2} have been reported for EFCs [6,7].

The low power output and short operating time of EFCs are issues currently being investigated. Various electrochemical tools are used to study the effects of construction materials, operating conditions, and other aspects of EFC operation. Among these tools is electrochemical impedance spectroscopy (EIS), which has been demonstrated in the literature as a useful tool for studying transport in PEMFCs, as well as in other types of fuel cells, including microbial fuel cells (MFCs). Although application of EIS to analyze EFCs has also been reported in recent literature, much more work remains to be done in this area to provide a better understanding of the dynamics of transport-related resistances in EFCs.

Mediators are commonly used in EFCs to transfer electrons between an electrode and a dissolved enzyme [5,8–11]. This design typically benefits from a three-dimensional electrode since the configuration greatly increases the electrode surface area for transfer of electrons to the mediator [3,6]. Tamaki and Yamaguchi [9] used EIS to study the effects of immobilizing mediators on the electrode surface. They found that modifications to the electrode did not significantly increase the internal resistance. The modifications

* Corresponding authors at: Oak Ridge National Laboratory, Oak Ridge, TN 37831, United States.
E-mail addresses: doug.aaron4@gmail.com (D. Aaron), borolea@ornl.gov (A.P. Borole), sotira.yiacoumi@ce.gatech.edu (S. Yiacoumi), tsourisc@ornl.gov (C. Tsouris).
[1] Tel.: +1 865 241 3246.

0378-7753/$ – see front matter. Published by Elsevier B.V.
doi:10.1016/j.jpowsour.2011.10.105

in their work actually sped up the oxidation of glucose by utilizing both mediated and direct electron transfer to the enzymes. In a study by Katz and Willner [11], EIS was used to individually study the anode and cathode of an operating EFC. Because the design of the EFC did not accommodate inclusion of true reference electrodes (such as Ag/AgCl or a standard hydrogen electrode), metal needles were included in the EFC to serve as quasi-reference electrodes. The cathode resistance was found to be approximately 70% of the total resistance. Single-electrode measurements were compared with whole-cell measurements. Danaee et al. [10] included adsorption in their EIS analysis of glucose oxidation on a single Ni-modified, glassy carbon electrode. They observed that the charge transfer resistance (CTR) decreased by nearly an order of magnitude when the glucose concentration increased from 1 mM to 7 mM. The resistance to glucose adsorption also decreased by a factor of 3 over this range of glucose concentrations. However, this experiment was not performed on an operating EFC. Instead, the phenomena that occurred at an electrode interacting with enzymes were studied.

Based on the similarity between EFCs and PEMFCs, it is apparent that EIS can be useful for studying transport phenomena in operating EFCs. In this work, internal resistance responses to operating conditions including enzyme concentration, air humidity, and airflow rate, as well as time-dependent studies, are presented. The goal of this study is to use EIS to identify the transport-limiting steps in the EFC in an effort to improve power density. A power density analysis is also included.

2. Experimental

2.1. EFC materials and design

A three-dimensional-cathode EFC reported by Borole et al. [6] was utilized in this work. The endplates were made of Lexan, and the gaskets were made of rubber. The cathode compartment was 0.325 cm thick with an open internal area of 1.8 cm × 1.3 cm. The anode compartment was approximately 0.075 cm thick with the same open internal area as the cathode. The anode material was 1 cm^2 Pt-deposited carbon cloth (Fuel Cell Store, Inc.). The cathode was made of carbon felt (Alfa Aesar) with an area of 1 cm^2 and thickness of 0.325 cm and 83% porosity. The carbon felt cathode was made hydrophilic via plasma treatment (Harrick Plasma Company). A Nafion 115 polymer electrolyte membrane (PEM) was used to separate the two electrodes. Loosely woven carbon cloth was included in both the anode and cathode to serve as a gas diffusion layer and to aid the contact with the current collectors. The anode current collector was made of graphite (same area as the anode compartment), while the cathode current collector was a gold wire in contact with the cathode gas diffusion layer. The cathode solution included the laccase enzyme from *Trametes versicolor* (Sigma, St. Louis, MO, 21.7 units (U) mg^{-1}), 100 mM citrate buffer at pH 4, and 2,2′-azinobis (3-ethylbenzothiazoline-6-sulfonate) (ABTS) as the mediator. For all experiments, the ratio of ABTS mediator to enzyme was maintained constant at 100:1. A schematic of the EFC is found in Fig. 1.

2.2. Electrochemical impedance spectroscopy

EIS was performed with a Gamry Series 750G potentiostat/galvanostat/zero-resistance ammeter. All measurements performed were two-electrode or whole-cell measurements since the EFC design did not accommodate the inclusion of a reference electrode. Inclusion of a reference electrode would be necessary for confirmation of individual electrode resistances, but it has been shown for similar systems that the enzymatic cathode dominates internal resistance [11]. The frequency range of the impedance spectra spanned from 100 kHz to 5 mHz with an ac amplitude of 1 mV; the frequency range resulted in scan times of approximately 15 min. Measurements were performed while the EFC was under a load of 500–1500 Ω. Fan et al. [12] have demonstrated that fuel cell output greatly influences EIS spectra.

Because the EFC is very similar in construction to the PEMFC, the same equivalent circuit model (ECM) often used for PEMFC EIS studies was used for analyzing the EFC spectra [13]. This ECM is composed of two parallel resistor–capacitor (R–C) elements that are in series with a single resistance (Fig. 2). As shown in Fig. 2, each R–C component represents an electrode while the center resistor represents a composite of "solution" resistances that includes the anode water layer, PEM, and cathode solution layer. The resistances at the electrodes are assumed to be dominated by charge transfer resistances. Also, at the electrode are constant phase elements (CPEs) that represent non-ideal capacitance occurring at the electrode–electrolyte interfaces. CPEs were used instead of ideal capacitors because the electrical double layers (EDLs) that form at this interface were not expected to develop ideal capacitance. Charge leakage, surface irregularities, and other non-idealities justify the use of CPEs. An exponent (termed "A factor") is used to modify the impedance of a capacitor in a CPE; this exponent can vary between 0 and 1 and describes the degree of non-ideality exhibited by the EDLs [14]. For a CPE, an A factor of 1 corresponds to an ideal capacitor while an A factor of 0 results in a completely non-ideal behavior. A diffusion impedance element was also considered in the ECM (Fig. 2) to account for transport of active species in the cathode; however, the model fit was not significantly improved, nor were the calculated resistances appreciably changed by the addition of the diffusion element. As such, the diffusion element was considered unnecessary for the ECM.

2.3. Operating conditions explored via EIS

EIS measurements were used to study the effects of various operating conditions on the power output and internal resistances of the EFC. The variables studied included enzyme loading, air saturation temperature, airflow rate, and salt concentration. Enzyme loadings were adjusted from 0.15 U/cm^2 to 15 U/cm^2; air-humidification temperature was varied from 25 °C to 50 °C; airflow rate was maintained between 10 sccm and 50 sccm; and salt concentration was varied between 100 mM and 800 mM. The air-humidification temperature was controlled by placing the humidifier in a thermostatically controlled hot water bath. The humidifier was a column filled with water through which the airstream was bubbled. Optimization of the conditions was expected to result in improved power density and longevity for the EFC. In general, greater enzyme loading, higher air saturation temperature, reduced airflow rate, and increased salt concentration were expected to contribute to EFC stability and, potentially, higher power output. Because of enzyme and mediator instability over time, as well as persistent loss of water, each experimental condition was performed with fresh enzyme solution and fresh EFC materials. Multiple runs of each experimental condition were performed to identify the degree of variability associated with rebuilding the EFC with fresh components.

3. Results and discussion

Since we are interested in transport limitations near optimal operation, EIS measurements were performed at the maximum power density for each EFC. In general, this corresponded to 750–1000 Ω external resistance, though some measurements were performed at 1500 Ω. The EIS spectra were difficult to model at low power density because of unstable impedance responses; thus,

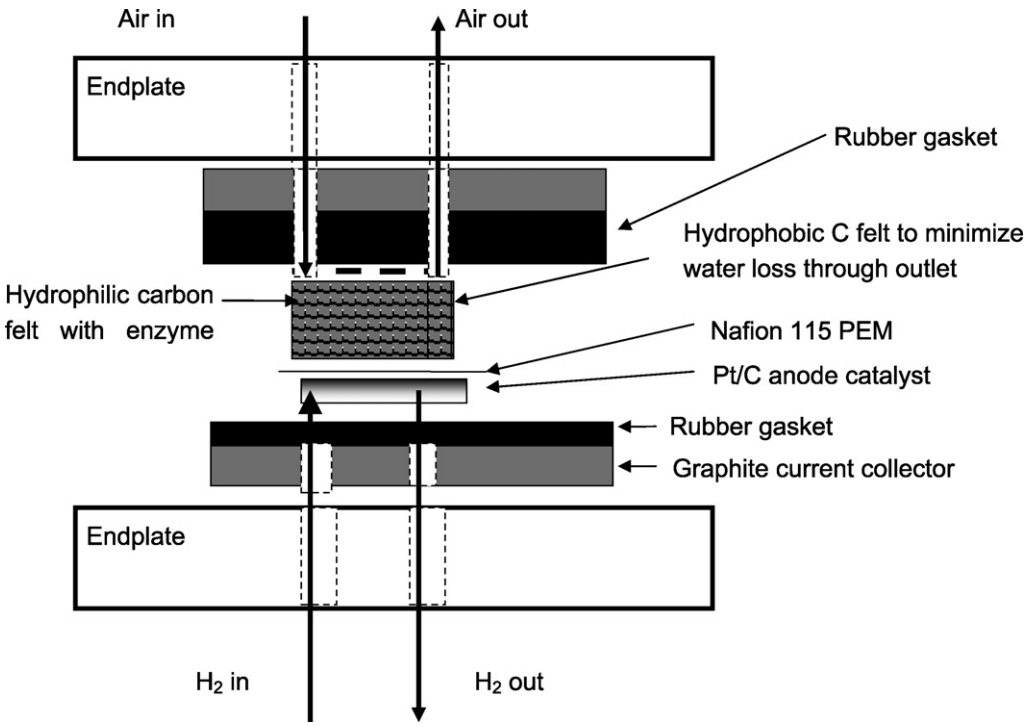

Fig. 1. Schematic of EFC used in the experiments in this work. All layers were held together via tie rods.

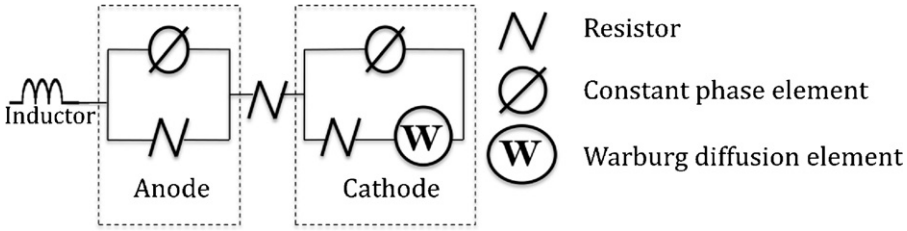

Fig. 2. Equivalent circuit model representing the EFC. The inductor accounted for behavior associated with the EIS cable and is thus not associated with phenomena that occurred within the EFC. The Warburg diffusion element proved to be unnecessary for good model fit.

most scans were performed at resistances that resulted in high power density. Because of drying observed in this work, as well as documented in other studies [5], the EFC power output decreased over time. This behavior presented problems with performing multiple EIS scans of the EFC (for reproducibility measurements). The measurements performed for varying air-side humidity were taken using multiple EFC builds. Each experimental setting was performed for multiple EFCs built with fresh materials, to check reproducibility. Each measurement took approximately 15 min to complete, and the output of the EFC was relatively stable between two consecutive sets of measurements. The time allowed before measurements after a change in conditions was approximately 2 h. Finally, because the inclusion of a diffusion impedance element did not improve model fit or appreciably change the calculated values for the electrode and electrolyte resistances, we do not report the diffusion impedance.

3.1. Effects of enzyme loading

The effect of enzyme loading was investigated for concentrations ranging from 0.15 U/cm^2 to 15 U/cm^2. Because the cathode was 1 cm^2, enzyme loading designations are simply 0.15 U, 15 U, etc. Enzyme loading was expected to have a strong influence on both power density and internal resistance since this parameter determined the amount of catalyst present in the cathode. In Fig. 3, Nyquist plots are included for enzyme loadings of 1, 10, and 15 U. Two results can be seen in the Nyquist plot: overall resistance and solution resistance decreased as enzyme loading increased. Generally, smaller Nyquist plots, as well as a lower local minimum at higher values of real impedance indicate reduced total resistance. We focus on the "total resistance" defined here as the sum of the real components of the impedance, namely the anode and cathode charge transfer resistances as well as the solution or electrolyte resistance. These points are marked as dotted lines in the inset in Fig. 3. Reduced solution resistance can also be seen in this inset: the high-frequency resistances for all three graphs decreased with increasing enzyme loading. These points correspond to the minimum real impedance exhibited by the plots. Table 1 lists the estimates of approximate solution and total resistances from Fig. 3. The solution resistance corresponded to the minimum x-intercept of each experimental spectrum (closest to the origin), while the total resistance was estimated as near the projected larger x-axis intercept (see dotted lines in inset in Fig. 3).

Table 1
Estimates of approximate solution and total resistances from Fig. 3.

Resistance (Ω)	1 U	10 U	15 U
Solution	13	7	4
Total	75	35	30

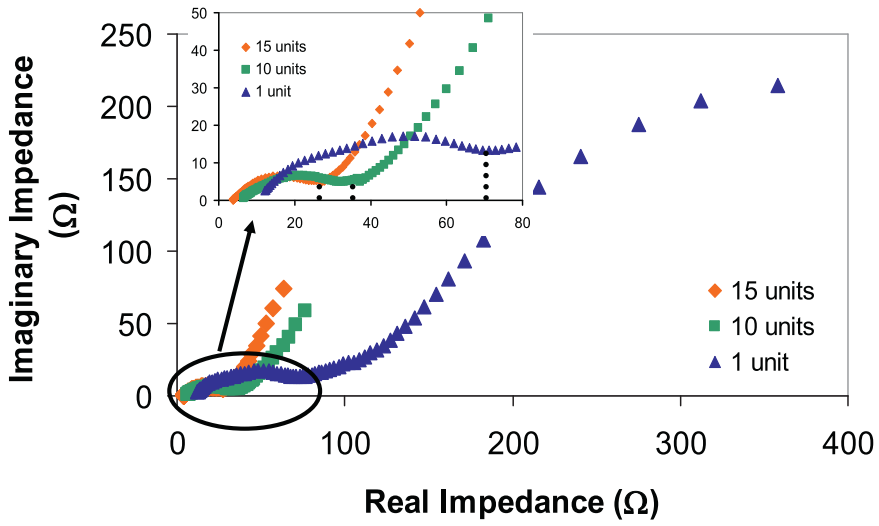

Fig. 3. Nyquist plots for varying enzyme loading in EFC cathode solution. The inset shows the high-frequency region for the results, illustrating the effect of enzyme loading on solution resistance and total resistance.

Lower overall resistance for greater enzyme concentration is reasonable since additional catalyst is present to speed up the oxygen reduction reaction in the cathode. The decrease in solution resistance with greater enzyme concentration may be related to proton transport. At an increased enzyme loading, because of a smaller effective electrode separation, more protons would more quickly meet laccase enzymes in the cathode, thus resulting in a reduced solution resistance. Another way of understanding this behavior is that the average time for protons to diffuse through the cathode water network before meeting a laccase enzyme is reduced when the enzyme loading is increased (i.e., more protons would encounter enzymes within the same time period in the cathode). This phenomenon is not common in PEMFC studies because the catalyst layer is of planar geometry; in an EFC, however, we have an intentionally three-dimensional cathode.

The ECM shown in Fig. 2 was utilized to break down the total real resistance into its constituent components of anode, solution, and cathode. The results for this modeling are included in Fig. 4. It is apparent that the resistance was dominant in the cathode even at the highest enzyme loading of 15 U. This result is in agreement with those found in the literature [5]. For the enzyme loadings studied, the cathode made up approximately 80% of the total resistance. Each measurement was performed for three independent EFCs. The variability in model-derived resistances was lower than 17% (the value for the cathode of the 15 U measurement) and was often below 5% between independent EFC builds. Cathode limitation is understandable since Pt was used in the anode and because no steps have been taken to optimize transport conditions in the cathode, other than to use a three-dimensional structure to facilitate airflow.

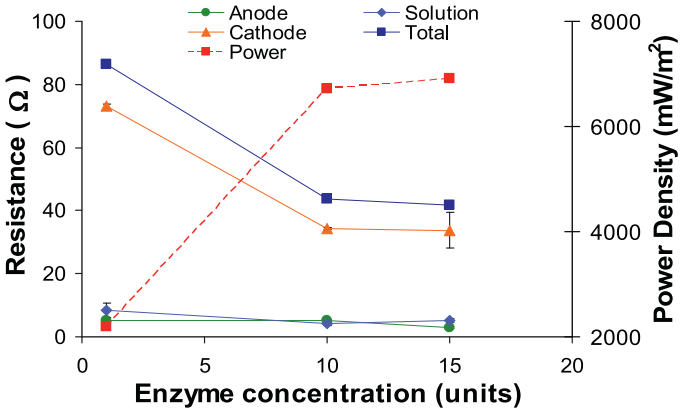

Fig. 4. ECM results for EFCs of varying enzyme loading in the cathode. The ratio of ABTS:laccase was held constant, as were all other experimental parameters.

Fig. 4 shows that most of the reduction in total resistance resulting from increases in the enzyme concentration occurred in the cathode. The cathode resistance decreased from approximately 87 Ω at 1 U loading to 41 Ω at 15 U loading, just over 50%. For the same increase in enzyme loading, the anode resistance decreased from 5 Ω to 3 Ω and the solution resistance decreased from 8.5 Ω to 5.1 Ω. Thus, improvement of the EFC cathode resulted in reduced transport resistances throughout the EFC.

The solution resistance exhibited a minimum of 4.1 Ω at 10 U enzyme loading. However, this phenomenon is believed to be more likely a systemic variance rather than a true trend of increased enzyme loading. System variability is considered a likely cause because the literature contains no indication that increased catalyst loading (for enzymes or Pt-based PEMFCs) somehow negatively affects solution resistance. Moreover, the Nyquist plots in Fig. 3 indicate that the solution resistance did decrease with increasing enzyme loading.

The total resistances shown in Fig. 4 were 86.5, 43.6, and 41.7 Ω for enzyme loadings of 1, 10, and 15 U, respectively. Thus, the total resistance was apparently reduced significantly when the enzyme concentration was increased from 1 U to 10 U but did not change much past this point. The maximum power density followed a similar trend: it increased from 2200 W m^{-2} to 6710 W m^{-2} when enzyme loading increased from 1 U to 10 U. However, increasing the enzyme concentration from 10 U to 15 U increased the power density to only 6900 W m^{-2}. These trends in total resistance and power density are shown in Fig. 4. For the system considered in this work, it appears as though little improvements in power density or internal resistance occurred when the enzyme concentration was increased above 10 U. Individual values for each of the resistances and enzyme loadings are shown in Table 2.

3.2. *Effects of operating resistance*

Experiments were also performed for enzyme loadings at multiple values of the external resistance. Our earlier experiments, as well as those in the literature [12], suggest that EIS responses are sensitive to the operating output of the fuel cell. As previously

Table 2
Impedance results from ECM modeling for experiments with varying enzyme loading.

Enzyme loading (U)	Anode (Ω)	Solution (Ω)	Cathode (Ω)	Total (Ω)	PD (mW/m^2)	Cathode% of total
1	5.0	8.5	73.0	86.5	2200	84.4
10	5.1	4.1	34.4	43.6	6710	79.0
15	2.9	5.1	33.7	41.7	6900	80.7

explained, a consistent basis was established by performing EIS at the maximum output of the fuel cell. The results from Fan et al. [12] indicate that the overall impedance of a fuel cell decreased with increasing current density. This finding is reasonable if one considers that the reaction rates are higher at a greater current. However, we found that the minimum total resistance was sometimes achieved at the maximum power density, rather than at the greatest current. Such behavior is illustrated in Fig. 5a and b. Fig. 5a qualitatively shows that the minimum internal resistance occurred at an external resistance setting of 500 Ω since that Nyquist curve is the smallest. Nyquist curves at 750 Ω and 1000 Ω show increasing total resistance. Other low-enzyme-loading experiments showed maximum power densities at very high external resistance settings (up to 3500 Ω). While the two Nyquist curves in Fig. 5b are similar, the 1000 Ω spectrum reached its first minimum at a lower impedance than the 750 Ω measurement (approximately 30 Ω compared with 44 Ω, respectively). Moreover, the second part of the 1000 Ω measurements began to curve back toward the *x*-axis before the 750 Ω measurements did. This trend was consistent among repeated spectra. Although enzyme/mediator degradation and water loss could have contributed to this occurrence, this is considered unlikely because the measurements were all performed within a 2 h period. Such phenomena could be the result of minimized charge transfer resistances at the electrodes, as well as reduction of other losses throughout the EFC.

The behavior described in the previous paragraph indicates the necessity of obtaining EIS data for fuel cells across a variety of operating conditions. Varying operating conditions for a fuel cell will certainly change its power output. Fig. 5a and b shows that the operating external resistance plays a role in the total resistance of the system; this resistance affects the current and potential of the fuel cell. Increased current (at low resistance) implies increased reaction rates at the electrodes and increased diffusion through the solution. Thus, resistances are minimized at high current densities. Such findings, however, are not truly relevant to the goal of fuel cell development. Power output is the primary aspect of fuel cell operation that will determine whether this technology can be useful for an application. As shown in this work, changing conditions can significantly affect the output of a fuel cell, by as much as an order of magnitude. At a first glance, it seems reasonable to compare all EIS results for identical output, and this is the approach that is often found in the EIS literature for fuel cells. However, by ensuring that the current densities are consistent, one neglects the power output aspect of a fuel cell, which is arguably the most pertinent consideration. Thus, EIS measurements were performed at maximum power densities in this work. The reasoning behind such a decision is that the maximum power density is what characterizes a fuel cell as an improvement over previous designs or ranges of operating conditions. Transport limitations at the maximum power density are, therefore, of primary interest.

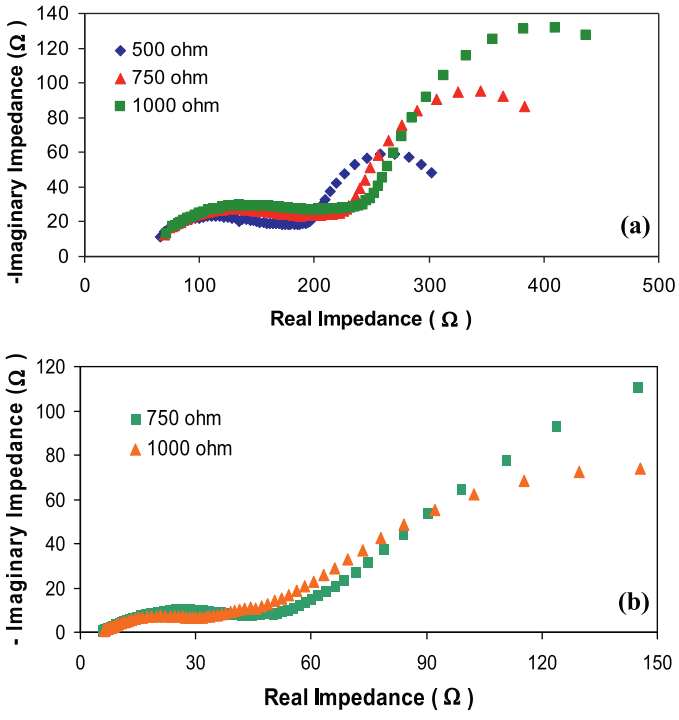

Fig. 5. (a) Nyquist plots for a 10 U laccase-loading EFC at three different external resistances. (b) Nyquist plots for a 0.30 U laccase-loading EFC at two different external resistances.

3.3. EFC behavior over time

EIS and power density measurements were performed on EFCs over time spans of approximately 24 h and 50 h. The EFCs had 10 U and 15 U loadings of laccase, respectively, with initial enzyme solution volumes of 100 μL. Measurements performed over time are of considerable interest since current EFCs are limited by a relatively short lifetime of less than a day until the enzyme solution (enzyme, mediator, buffer, and water) must be refreshed. In this work and that of others [5], it has been noted that water loss is a significant problem, occurring even when a saturated airstream is used. The water content in these experiments was monitored at the beginning and termination of the experiment by weighing the carbon felt; water loss as high as 15% consistently occurred within a period of 4 h. Since water provides the medium for transporting protons from the anode to the cathode, as well as for ABTS to shuttle electrons from the electrodes to the laccase enzyme, loss of water is believed to have contributed to the loss of power output over time. EIS experiments performed by Hudak et al. [5] have shown that the solution resistance in EFCs increased over time, even when a humidified airstream was fed to the cathode. However, humidification did significantly reduce the rate at which the solution resistance increased, indicating a reduction in water loss rate. In addition to water loss, the enzymes and mediator can also degrade over time. All three of these mechanisms contribute to the loss of power for an EFC over time. In general, it is assumed here that increased solution resistance is linked to water loss, while all three mechanisms contribute to increased resistance at the electrodes (though enzyme and mediator degradation occur only at the cathode). Thus, if no change in solution resistance were observed, degradation of enzyme and mediator would likely be the primary cause of power loss.

Fig. 6 shows trends in each individual resistance, as well as in the overall resistance for a 10 U EFC over 49 h of operation. Over the course of the experiment, the cathode resistance increased

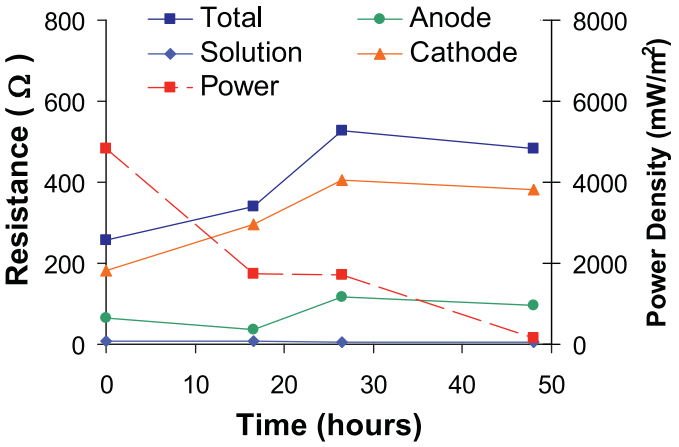

Fig. 6. Internal resistance results from ECM analysis for a 10 U EFC operated for 49 h at a constant load with fully humidified air and hydrogen streams.

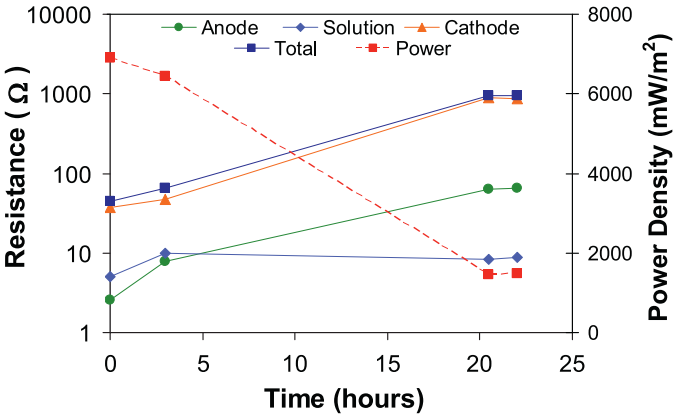

Fig. 7. ECM results for 15 U EFC operated over 22 h at a constant load. Note that the *y*-axis is logarithmic because of a large increase in resistance after ~20 h.

substantially; the anode resistance increased slightly; and the solution resistance was relatively unchanged. Nafion is well known to persistently retain water, thus the consistent solution resistance is reasonable. These results suggest that phenomena occurring in the cathode, such as water loss and enzyme or mediator degradation, were the primary cause of the increase in the total internal resistance of the fuel cell. The fact that water loss occurred in the cathode was recently confirmed by neutron imaging experiments [15]. Furthermore, neutron imaging was used to quantify the rate of water loss in the cathode. Here, EIS provided information that can be used to determine which degradation mechanism is more likely to be causing loss of power.

Fig. 6 shows power density and total resistance over time for the 10 U EFC experiments that were analyzed via the ECM in Fig. 2. It is apparent that the power density decreased significantly over the first 17 h to approximately 33% of the initial power output, from 4800 mW/m^2 to 1740 mW/m^2. After 49 h, the power density was only 220 mW/m^2, and the total resistance increased to 480 Ω. A local maximum in resistance occurred at 27 h, but this behavior was not reproducible. It is possible that a water droplet condensed in the line and entered the cathode sometime after 27 h. Had this occurred, the water content in the cathode would have increased; such an increase in water content can lower the resistance in the EFC as indicated by Hudak et al. [5]. Continuous drying was expected in the cathode. However, entry of a water droplet would allow for lower total resistance, resulting in a local maximum as seen in Fig. 6. We have observed in previous work that a water droplet can enter the cathode, which results in significantly increased power output [15]. Although the results presented in this section can explain power loss in the EFC over time, it is still difficult to separate the contributions of water loss from those of enzyme and mediator decay.

Another EFC of similar construction was built and run overnight with 15 U enzyme loading, 10 sccm air and hydrogen flow rates, and saturation of both feed streams. The results from this EFC were interesting because the changes in total resistance and power density were much greater than those of the 10 U EFC reported above. As seen in Fig. 7, the total resistance increased from 45 Ω to 965 Ω after 22 h, a 21-fold increase in resistance. For comparison, the total resistance for the 10 U EFC increased by only a factor of 2. Moreover, this 15 U EFC exhibited greatly increased anode resistance over the course of the experiment whereas the anode was relatively stable in the 10 U EFC. As shown in Fig. 7, the anode resistance increased from 2.6 Ω to 65 Ω over 22 h. During this same period, the cathode resistance increased from 37 Ω to 865 Ω. The solution resistance for this run varied between 5 Ω and 10 Ω. The increase in anode and solution resistances could be a result of the slowdown of the cathode reaction, which would have adverse effects on the rest of the interrelated processes occurring in the EFC.

Fig. 7 also shows total resistance and power density over the 22 h experiment with the 15 U EFC. While the resistance increased by a factor of 21, the power density decreased from 6892 mW/m^2 to 1478 mW/m^2—a loss of 79% power output. Internal resistance and power density do not always vary in an inversely proportional fashion (i.e., twice as much resistance does not result in half the power output). This occurs because the resistances measured here do not include all internal impedances, since capacitances and inductances, as well as resistances, influence impedance. However, impedance and power output are inversely related.

The changes observed in the EFC over time are likely attributable to a combination of drying, mediator loss, and enzyme loss. Aaron et al. [15] performed in situ water loss measurements without interrupting cell operation via neutron imaging. Measurement of the enzyme and mediator activity at the end of an experiment would be beneficial to better understand the mediator and enzyme losses with time. Because the method of enzyme solution distribution in the cathode carbon felt was not uniform, the drying behavior was not expected to have been uniform either. Thus, deposits of enzymes and mediator would be more concentrated in some places of the carbon felt than in others. Of the three loss mechanisms, water content is the most easily measured and the only parameter that could be quantified in situ so far via neutron imaging.

3.4. Effects of air-humidification temperature

Water loss has been identified as a significant limitation with regard to EFC longevity. One method to decrease the rate of water loss is to humidify or supersaturate the airstream being fed to the cathode [5]. With greater water content in the airstream, the driving force for evaporation from the cathode should be reduced. Improved water retention should then result in a more stable power output. Experiments were, therefore, performed at humidifier temperatures ranging from 25 °C to 50 °C. All other experimental parameters (enzyme loading, feed flow rates, etc.) were maintained constant. Measurements were taken approximately 30–60 min after attaching feeds to the EFC to minimize the effects of degradation between runs.

Fig. 8 shows ECM results for the 10 U EFC at varying air-humidification temperatures. An overall relationship between temperature and total resistance is noted: the total resistance decreased from 51 Ω at 25 °C to 43 Ω at 50 °C. Little net change occurred in the anode, while an increase in solution resistance was observed (from 4.10 Ω to 5.95 Ω as the temperature increased

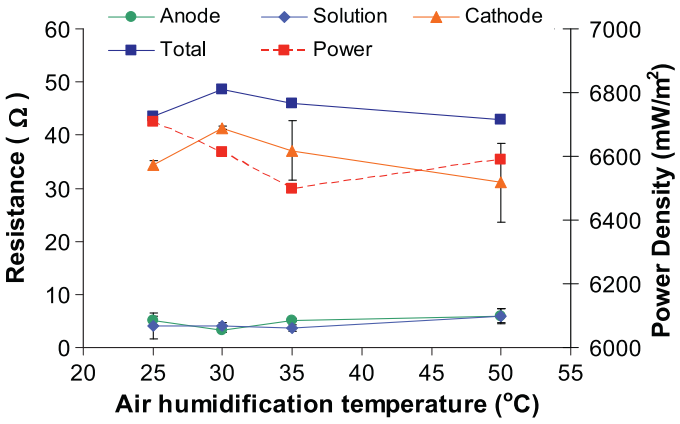

Fig. 8. ECM results for a 10 U EFC for experiments with humidification temperature ranging from 25 °C to 50 °C.

from 25 °C to 50 °C). The increase in solution resistance was within the error boundaries; however, it is unclear whether an inverse relationship would exist between humidification temperature and solution resistance. The power output for the EFCs run at the various temperatures did not exhibit a consistent trend, nor did it vary widely. Thus, humidification temperature seemed to minimally affect power output. Most catalytic processes occur more rapidly at elevated temperatures, because more collisions per time would occur between the substrates and catalysts. In this case, enzymes, oxygen, protons, and mediators must come together to perform the oxygen reduction reaction and form water. It is apparent that the air-humidification temperature did not greatly affect power output or internal resistances. However, the effect of air-humidification temperature is expected to be significant for EFC output stability and water retention in the cathode.

4. Conclusions

In this work, multiple aspects of EFC construction and operation were studied via EIS. Of these conditions, enzyme loading, external resistance (and operating current), air humidification, and stability over time were of interest. Enzyme loading was found to have a very strong influence on both power density and internal resistances. As enzyme loading increased, the oxygen reduction reaction proceeded at a more rapid rate, contributing to a significant reduction in cathode resistance. The external resistance, as noted elsewhere [12], affected the EIS parameters studied in this work. Contrary to findings in some other studies [12], however, the maximum current density did not always coincide with minimum total internal resistance. Thus, it was decided that EIS would be performed at maximum power density since this is the most pertinent feature of a fuel cell. Air humidification did not strongly affect the resistances or power output of the EFC; however, some reduction in internal resistance was observed as the humidification temperature was elevated. This reduction is attributed to more thermal energy in the cathode, accelerating the catalytic reaction that occurs in the cathode. Also studied was the EFC stability over time. Significant power loss occurred over the first 16 h of operation, though power loss was observed as quickly as 4 h after connection to the feed streams.

Acknowledgments

This work was supported by the American Chemical Society, Petroleum Research Fund–Green Chemistry Initiative at Georgia Institute of Technology. EFC work at Oak Ridge National Laboratory was supported by the Laboratory Directed Research and Development Program of ORNL. Oak Ridge National Laboratory is managed by UT-Battelle, LLC, for the U.S. Department of Energy under contract DE-AC05-00OR22725.

References

[1] P. Atanassov, C. Apblett, S. Banta, S. Brozik, S.C. Barton, M. Cooney, B.Y. Liaw, S. Mukerjee, S.D. Minteer, Electrochemical Society Interface 16 (2007) 28–31.
[2] R.A. Bullen, T.C. Arnot, J.B. Lakeman, F.C. Walsh, Biosensors & Bioelectrontronics 21 (2006) 2015.
[3] S.D. Minteer, B.Y. Liaw, M.J. Cooney, Current Opinion in Biotechnology 18 (2007) 1–7.
[4] A. Zebda, L. Renaud, S. Tingry, M. Cretin, F. Pichot, R. Ferrigno, C. Innocent, Sensor Letters 7 (2009) 824–828.
[5] N.S. Hudak, J.W. Gallaway, S.C. Barton, Journal of the Electrochemical Society 156 (2009) B9–B15.
[6] A.P. Borole, S. LaBarge, B.A. Spott, Journal of Power Sources 188 (2009) 421–426.
[7] W. Gellett, J. Schumacher, M. Kesmez, D. Le, S.D. Minteer, Journal of the Electrochemical Society 157 (2010) B557.
[8] T. Samukawa, S. Tsujimura, K. Kana, Bunseki Kagaku (2008) 625–629.
[9] T. Tamaki, T. Yamaguchi, Industrial & Engineering Chemistry Research 45 (2006) 3050–3058.
[10] I. Danaee, M. Jafarian, F. Forouzandeh, F. Gobal, M.G. Mahjani, Electrochimica Acta 53 (2008) 6602–6609.
[11] E. Katz, I. Willner, Journal of the American Chemical Society 125 (2003) 6803–6813.
[12] Y. Fan, H. Hu, H. Liu, Journal of Power Sources 171 (2007) 348–354.
[13] D. Aaron, S. Yiacoumi, C. Tsouris, Separation Science and Technology 43 (2008) 2307–2320.
[14] Gamry Instruments, Application Note, Basics of Electrochemical Impedance Spectroscopy, Rev. 1.0, 9/3/2010, www.gamry.com/App_Notes/Index.htm (date accessed 10.5.2010).
[15] D.S. Aaron, A.P. Borole, D.S. Hussey, D.L. Jacobson, S. Yiacoumi, C. Tsouris, Journal of Power Sources 196 (2011) 1769.